Liquid Metal-Assisted Acylation of Phenols over Zeolite Catalysts

Yong Zhou, Geqian Fang, Deizi Peron, Maya Marinova, Vladimir Zholobenko, Andrei Khodakov, Vitaly Ordomsky

Liquid Metal-Assisted Acylation of Phenols over Zeolite Catalysts

Yong Zhou [a,b], Geqian Fang [a], Deizi Peron [a], Maya Marinova [c], Vladimir Zholobenko [d,e], Andrei Y. Khodakov [a]*, Vitaly V. Ordomsky [a]*

[a] *Univ. Lille, CNRS, Centrale Lille, Univ. Artois, UMR 8181 - UCCS – Unité de Catalyse et Chimie du Solide, F-59000 Lille, France.*

[b] *Research Institute of Interdisciplinary Sciences (RISE) and School of Materials Science & Engineering, Dongguan University of Technology, Dongguan 523808, China*

[c] *Institut Michel-Eugène Chevreul, 59655 Villeneuve-d'Ascq, France*

[d] *Department of Chemistry, Moscow State University, Lenin Hills, 119892 Moscow, Russia*

[e] *School of Physical and Chemical Sciences, Keele University, ST5 5BG, Staffordshire, UK*

Corresponding author: Andrei Khodakov (andrei.khodakov@univ-lille.fr), Vitaly V. Ordomsky (vitaly.ordomsky@univ-lille.fr)

Abstract

The selection of a solvent for the reaction is highly important in catalysis since it profoundly affects the catalytic activity, selectivity, and stability. However, the costly separation of solvent from the products hinders the application of solvents in industry. In this study, we propose the utilization of liquid metals to regulate the catalytic performance of non-metallic zeolite catalysts. The catalytic reactions of phenols acylation over heterogeneous acidic BEA zeolite were conducted in the presence of liquid metal alloys above their melting points. The presence of liquid metals in the reaction medium leads to dramatic change of the selectivity toward ester formation for the phenol acylation reactions at high stability of the catalyst. The observed phenomena were attributed to a strong interaction of the liquid metal with the catalysts, resulting in the modification of the strength of zeolite acid sites and to a decrease in the residence time of the products on the surface of the catalyst.

Keywords: Liquid metal, solvent, acylation, stability, selectivity

Introduction

The solvent selection plays an important role in both homogeneous and heterogeneous catalytic reactions. In the case of homogeneous catalysis, the solvent may affect the intermediate states with a decrease in the reaction activation energy [1]. The proper solvent can shift the reaction selectivity to a target product.[2] The effect of solvent on heterogeneous catalysis is more complex because it involves interfacial effects, competitive adsorption and mass transfer, [3, 4] etc. Therefore, it makes less predictable solvent effect on activity, selectivity, and stability.

Depending on the type of reaction, the solvent can strongly interact with catalysts [5, 6] or be inert, for example, in the case of extraction of some types of products [7]. Strong interaction of the catalyst with solvent and low interaction with reagents has recently been proposed as a way to merge the advantages of homogeneous and heterogeneous catalysis.[8] For example, ionic liquids with very low volatility in the form of separate phases or coated over support (Supported Ionic Liquid-Phase, SILP) have been efficiently used for different catalytic applications [7, 9-11]. However, the limited thermal stability of the liquid organic salts (< 200 °C) and leaching of the ionic liquid during the reaction significantly restrict their application in catalysis.

In comparison with organic solvents, liquid metals (LM) can be used with fewer temperature limitations. LM is a rapidly developing area for different applications [12-16]. Low melting point, easy recovery, high mobility, and surface energy are the main advantages of LM for catalysis. It is reported that bimetallic catalysts based on supported Ni, Pd, and Pt promoted with Ga have demonstrated high selectivity, activity, and stability in hydrogenation and dehydrogenation reactions [17-19]. The reaction proceeds on the intermetallic surface with modification of the electronic structure and

isolation of metal active sites. Our recent results have demonstrated that the presence of pseudoliquid Bi and Pb films on the surface of Fe and Co catalysts results in significant enhancement of selectivity, activity, and stability in high- and low-temperature Fischer-Tropsch synthesis [20-22]. The effect has been ascribed to the high mobility of the Bi and Pb promoters, which facilitate CO dissociation by scavenging O atoms and improving the stability of metal nanoparticles.

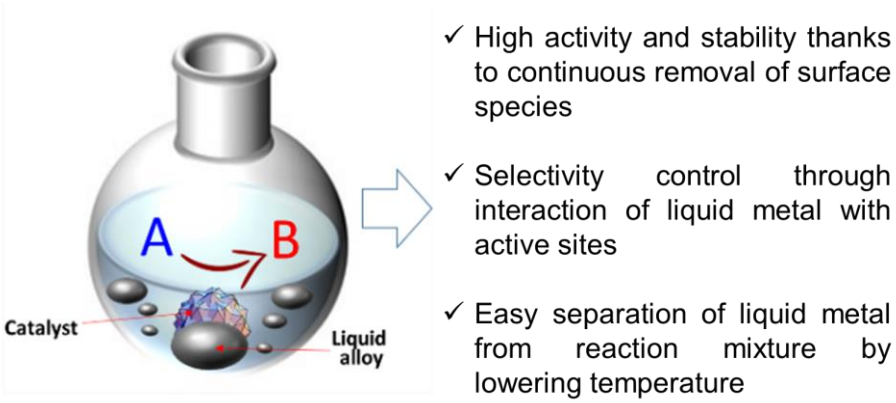

Figure 1. *Proposed concept of using LM as a reacting medium in heterogeneous catalysis.*

The disadvantage of catalyst promotion with small amounts of liquid metals is its limitation to metal-based catalytic reactions [23, 24] and possible aggregation of liquid metal promoters and catalyst active sites during the reaction or catalyst activation. A possible way to provide permanent contact of the catalysts with liquid metals would be the presence of the liquid metal phase not only on the specific areas of catalyst surface but in the catalytic reactor (**Figure 1**). Currently, LM in pure phase has been mainly used for the synthesis of materials such as thin oxides,[25, 26] nanowires,[27] etc. It can be suggested that continuous interaction of the catalyst with the liquid metal phase would affect the elementary steps of the reaction and overall catalytic performance (**Figure 1**).

In this work, we propose a novel concept for controlling the activity, selectivity of catalytic reactions and catalyst stability in the presence of LMs (**Figure 1**). This concept

involves conducting catalytic reactions in LM, which plays a role of reaction medium in the batch reactor. The acylation reaction over the zeolite catalyst serves as a model reaction to verify this concept. The acylation of alcohols and phenols is one of the key and fundamental reactions for the synthesis of pharmaceuticals, polymers, cosmetics, and perfumes [28]. Acid anhydrides have been the most commonly used reagents in homogeneous acid-base catalysis[29]. With the extensive development of heterogeneous systems, solid acid catalysts, such as zeolites, were exploited for the esterification of carboxylic acids with alcohols and phenols [30, 31]. However, low yield due to hydrolysis of the product over acid sites, low selectivity due to side reactions of C-acylation, and fast deactivation by adsorbed acylated products are serious drawbacks of the current state-of-the-art processes [32]. An excess of organic solvent and alcohol is usually needed to provide a high yield of the product. In this concept-proof investigation, a strong interaction of catalysts with liquid metal was uncovered, resulting in the modification of the acid sites of zeolites. The presence of liquid metal in the reaction medium leads to higher activity, stability, and selectivity toward ester formation for the acylation reactions.

Experimental Section

Materials

BEA zeolite with SiO_2/Al_2O_3 ratio of 25 was supplied by Zeolyst (CP841E*). The PbSn alloy (Pb 37% - Sn 63%, eutectic, 183 ℃) was purchased from FCT Solder. Wood's metal alloy (Bi 50% - Pb 25-26.7% - Sn 12.5-13.5% - Cd 10-12.5%, eutectic, 70-74 ℃), BiSn alloy (Bi 58% - Sn 42%, eutectic, 138 ℃) and BiSnAg alloy (Bi 57% - Sn 42% - Ag 1%, eutectic, 139-140 ℃) were purchased from Haines & Maassen Metallhandelsgesellschaft mbH. Phenol (99%); resorcinol (99%); 1-naphthol (99%);

hexanoic acid (99%), benzoic acid (99.5%) and biphenyl (99.5%) were purchased from Sigma-Aldrich.

Wood's/BEA was prepared by mixing 0.2 g of BEA with 0.2 g of Wood's metal powder and heating the mixture with intensive stirring at 175 ºC for 3 h. PbSn/BEA was prepared by mixing 0.2 g of BEA with 0.2 g of PbSn powder and heating the mixture with intensive stirring at 200 ºC for 3 h.

Catalyst Characterization

Electron micrographs were obtained using a ZEISS EVO 18 scanning electron microscope (SEM) equipped with EDS analysis by Oxford INCA ENERGY X-Max 20. For TEM analysis, a JEOL-2011F was used that had an acceleration voltage of 200 kV. Before TEM characterization, the samples were dispersed in an ethanol solution with ultrasonic treatment for 30 min and then dropped onto a carbon film on a copper grid. The STEM-EDX mapping was performed on a TITAN Themis 300 S/TEM microscope equipped with a probe aberration corrector, allowing a spatial resolution of 70 pm, a super-X windowless 4 quadrant SDD (silicon drift detector) detection system for STEM-EDX mapping and several annual dark field detectors.

The ammonia temperature programmed desorption mass spectrum (NH_3-TPD-MS) of the catalysts was evaluated using an AutoChem II 2920 apparatus (Micromeritics). The samples (100 mg) was saturated by ammonia at 100 °C, flushed with He and heated to 800 °C with a temperature ramp of 10 °C/min.

Thermogravimetric analysis (TG) measurements were performed using a SDT 2960 analyzer from TA instrument under air flow (50 ml/min) with a temperature increase rate of 10 °C/min. The chemical composition of the sample was determined by X-ray fluorescence (XRF) on a M4 TORNADO spectrometer (Bruker).

Low-temperature N_2 adsorption-desorption experiments were performed on a Micromeritics Tristar Model 3020 Surface Area and Porosimetry analyzer. 100 mg of the sample was degassed under a vacuum for 250 ℃ for 2 h, and then N_2 was used as adsorbate. The nitrogen isotherms were measured at -196 ℃. Micropore volumes (V_{mic}), microporous surface (S_{mic}) and external surface area (S_{ext}) were determined using a t-plot method.

Before FTIR studies, the zeolites were pressed into self-supporting discs (1.3 cm in diameter, S=1.3 cm^2; 10 - 15 mg/cm^2) and pretreated in situ in an IR cell at 450 °C under vacuum (1 ℃/min temperature ramp; 10^{-5} Torr) for 5 h. Adsorption experiments with different probe molecules were monitored using a Thermo iS10 spectrometer equipped with a DTGS detector at a spectral resolution of 4 cm^{-1}. An excess of probe molecules was introduced into the IR cell and the physisorbed species were removed by evacuation at the adsorption temperature. Adsorption of 1,3,5-triisopropylbenzene (TIPB, $C_{15}H_{24}$, Sigma-Aldrich, 95%) was carried out at room temperature. Pyridine (Py, C_5H_5N, Acros Organics, 99.5%), was adsorbed at 150 ℃. Physiosorbed Py molecules were subsequently removed by evacuation at 150 ℃. The infrared spectra obtained were analyzed (including integration, subtraction, and determination of peak positions) using specialized Thermo software, Omnic 9.3. For the quantification of the acidic properties of zeolite using adsorbed pyridine FTIR spectra, the following molar absorption coefficient values were applied: ε(BAS)=1.16 cm μmol^{-1} for Brønsted acid sites (BAS, IR peak at ~1545 cm^{-1}) and ε(LAS)=1.71 cm μmol^{-1} for Lewis acid sites (LAS, IR peak at ~1455 cm^{-1}) [33]. Some FTIR spectra were also recorded using a Thermo Fisher Scientific Nicolet 6700 FTIR (32 scans at a resolution of 4 cm^{-1}) equipped with

a mercury cadmium telluride (MCT) detector.

Catalytic Tests

Before being used as catalysts, BEA zeolite samples were activated in an oven at 550 ℃ for 6 h. Most part of phenol acylation with hexanoic acid on BEA zeolites with and without the presence of liquid metal alloy was performed at atmospheric pressure in Radley parallel glass reactor tubes with rotation at 500 rpm. Some experiments were conducted using WPR-series parallel reactor tubes (Nanjing Wen'er Instrument Equipment Co., Ltd.).

In a typical run, phenols (phenol, resorcinol or 1-naphthol) 10 mmol, acylating agent (hexanoic acid or benzoic acid) 10 mmol, BEA zeolite 0.2 g were added to the glass reaction. Subsequently, in experiments involving the presence of a liquid metal alloy, 4 g of the liquid metal alloy was added. The reaction mixture was heated to 190 °C for PbSn alloy and 175 ºC for Wood's metal, BiSn and BiSnAg alloys under reflux conditions. The samples of phenol acylation were taken from the reaction mixture for analysis in GC periodically. Biphenyl was used as an internal standard. The products of the reaction were analyzed by GC (Agilent Technologies 7820A) equipped with a HP-5 polar column and a flame ionization detector (FID), with an inlet temperature of 250 ºC. GC-MS analysis (Agilent Technologies 5977A MSD with Agilent Technologies 7890B GC system equipped with the HP-5 capillary column) was used to identify the organic compounds.

The conversion of phenols, selectivity, and yield to the corresponding products were defined as follows:

Conversion (%) = $1 - \frac{n_A}{n_A^o}$

Selectivity to the product p (%) = $\frac{n_p}{n_A^o - n_A}$

Yield (%) = Conversion × Selectivity

n_A , n_A^o and n_p refers to the final, initial moles of the reagent and the final moles of the product multiplied by the amount of reagent units in the molecule, respectively. Biphenyl was used as an internal standard for the GC analysis. The carbon balance carried out with biphenyl as the standard was better than 90 %.

Results and discussion

1. Acylation of phenol in the presence of LM

Commercial BEA zeolite with a SiO_2/Al_2O_3 ratio of 25 has been used for phenol acylation by hexanoic acid. The reaction is fast at the beginning with slowing down of the reaction rate over time. The reaction proceeds with high selectivity to O-acylated (phenylhexanoate) product with subsequent growth of the contribution of C-acylated (1-(2-hydroxyphenyl)hexan-1-one and 1-(4-hydroxyphenyl)hexan-1-one) products with reaction time due to Fries rearrangement over the acid sites with an approximately equal contribution of each of them after 3 h of test (**Figure 2, Figure S1, SI**)[34]. The selectivity to the C-acylated products decreases in the row: ortho>para, which corresponds to the thermodynamic equilibrium [35].

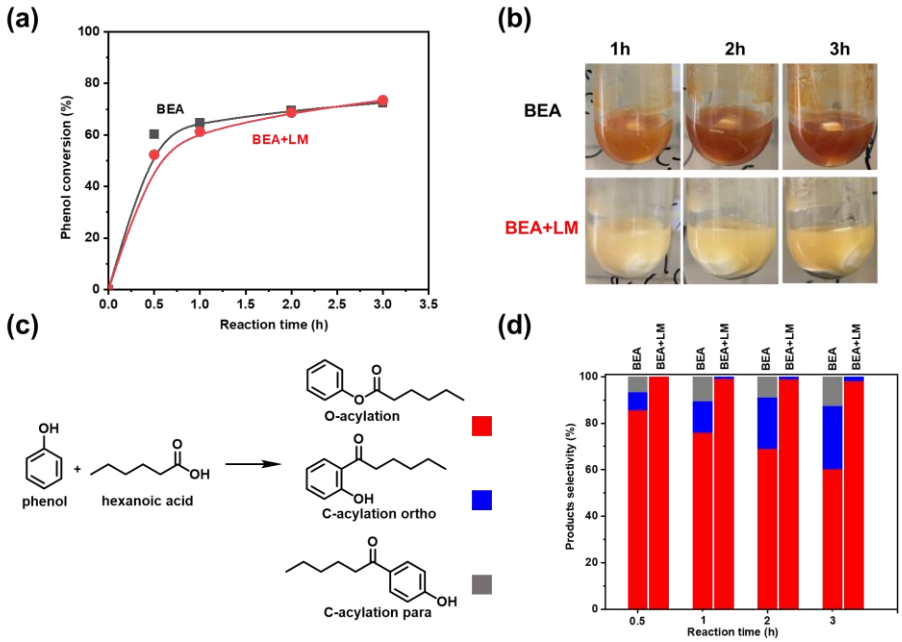

Figure 2. *Phenol acylation by hexanoic acid over BEA zeolite with and without adding LM in the reactor. (a) Phenol conversion as a function of reaction time, (b) Photos of reaction mixtures during reaction, (c) Scheme of the reaction and (d) Product selectivities in time. Reaction conditions: phenol, 10 mmol; hexanoic acid, 10 mmol; BEA zeolite, 0.2 g and Wood's alloy, 4 g; 175 °C.*

In other sets of experiments, the reaction was conducted in the reactor filled with the soldering Wood's metal alloy with a melting point of 70 °C. The LM alloy itself was inactive in acylation. The catalytic test in the presence of the LM alloy results in a spectacular shift in selectivity toward the O-acylation product (**Figure 2**). A selectivity to phenyl hexanoate higher than 98% was achieved. Interestingly, the presence of LM does not affect the reaction rate with time (**Figure 2a**).

Furthermore, phenol acylation with hexanoic acid in the presence of other LMs, such as BiSn, and BiSnAg alloys was investigated (**Figure 3**). With LMs, exceptionally high selectivity to the O-acylated product, phenyl ester was observed. Some decrease

in phenol conversion was observed after adding BiSn and BiSnAg alloys.

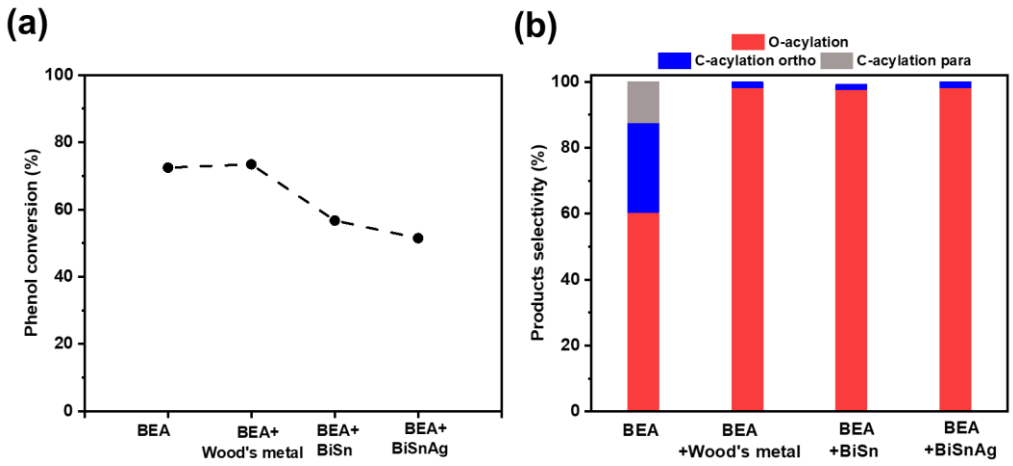

Figure 3. *The conversion (a) and product selectivity (b) of phenol acylation by BEA with different types of LMs. Reaction conditions: phenol, 10 mmol; hexanoic acid, 10 mmol; BEA zeolite, 0.2 g and LM, 4 g; 175 °C; 3 h.*

To explore the scope of utilizing LM to promote catalytic performances, acylation of phenyl derivatives with both hexanoic acid and benzoic acid was studied under similar conditions. As shown in **Figure S2, SI** and **Figure 4**, a high phenol conversion of up to 70% with both hexanoic acid and benzoic acid was observed over the BEA + Wood's metal system which is comparable and even better than for the zeolite without liquid metal. Notably, a substantial increase in the production of O-acylated products, such as phenyl esters, was observed. The catalyst system containing LM also demonstrated significant efficiency in the acylation of other substances, such as resorcinol and 1-naphthol, possessing either more electron-donating hydroxyl groups or a larger molecular size, respectively. Compared to phenol, resorcinol is richer in electrons and showed higher conversion in both acylation reactions, with C-acylation products, aryl ketones, being the main products. In particular, when hexanoic acid was

used as an acylating agent, 1-(2,4-dihydroxyphenyl)hexane-1-one was the dominant product with a selectivity of up to 90 % (**Figure S2, SI**). The addition of LM to the reactor resulted in a significant shift of the selectivity to O-acylated phenyl esters. Impressively, with benzoic acid as an acylating agent, in the presence of LM, the selectivity to the O-acylated product, reached 100 %. Furthermore, 1-naphthol was selectively acylated to phenyl esters in the presence of wood's metal, giving 94.5 and 98 % selectivity to phenyl ester with hexanoic acid and benzoic acid as acylating agents, respectively. The moderate decrease in 1-naphthol conversion was possibly due to the increased steric hurdle caused by the interaction of LM with acid sites of zeolites.

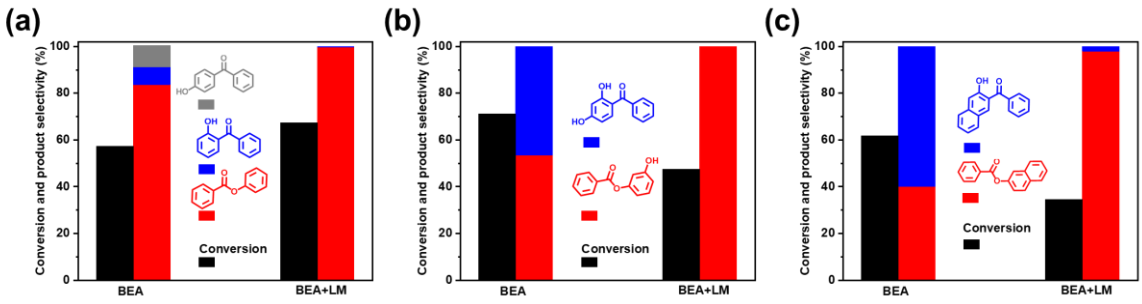

Figure 4. *LM promotes the acylation of phenols (phenol (a), resorcinol (b), and1-naphthol (c)) with benzoic acid over BEA zeolite. Reaction conditions: phenols, 10 mmol; benzoic acid, 10 mmol; BEA zeolite, 0.2 g and Wood's metal alloy, 4 g; 175 °C; 3 h.*

Noticeably, the reaction mixture in the conventional catalytic test was dark compared to the white colour observed in the catalytic test in the presence of LM (**Figure 2**). The dark colour could be attributed to the zeolite deactivation, which probably contains deposed carbon species. The effect is more obvious at 190 °C using PbSn alloy with a melting point at 183 °C (**Figure S3, SI**). The catalyst test for several

cycles over BEA without added LM with intermediate catalyst and product separation demonstrates a rapid decrease in activity with almost full deactivation after three cycles (**Figure S4, SI**). On the contrary, no visible deactivation after several cycles was observed when the BEA zeolites operated in LM.

The observed catalytic effect could be due to the zeolite modification by LM in the first cycle. In order to verify this assumption, the catalyst exposed to LM in the first cycle has been used in the absence of LM alloy in the second and third reaction cycles. It is interesting to note that the catalyst operating without LM still deactivates in the second and third cycles, while the selectivity shifts back to the C-acylated product (**Figure S4, SI**). It means that presence of LM in the reactor is indispensable for the selectivity and stability effects.

TGA, FTIR, and GC-MS analyses of extracted compounds have been used for the identification of carbon species present after catalytic tests in the zeolite catalyst (**Figure S5-S7, SI**). The oxidation of deposed carbon species in BEA zeolite after reaction without LM proceeds in a temperature range of 400 to 600 °C, with a weight loss of 19 wt. % (**Figure S5, SI**). At the same time, the BEA catalyst after reaction in the presence of LM contains only about 6 wt. % deposed carbon. The FTIR (**Figure S6, SI**) and GC-MS (**Figure S7, SI**) indicate the presence of multi-acylated products in the deactivated BEA zeolite, which could block the catalyst pores. The deactivation of the zeolite catalysts during phenol acylation in gas phase by acetic acid has been previously observed and assigned to generation of o-hydroxyacetophenone, which forms heavier compounds via condensation reactions [36].

Thus, the presence of a liquid alloy in the reactor leads to modification of the selectivity and significant improvement of the stability of zeolite catalysts in the acylation of phenol by hexanoic acid to the O-acylated products. The weight ratio of the PbSn alloy to the substrate was varied from 0.1 to 4 to investigate the effect of the LM content on the reaction performances (**Figure S8, SI**). As expected, less significant modifications of the selectivity compared with those of the parent catalyst were observed in the presence of smaller amounts of LM. The increase in the LM content in the reactor results in a gradual increase in the selectivity to O-acylated products.

The phenol conversion and acylation selectivities measured at different stirring rates are shown in **Figure S9, SI**. Note that the stirring rate has a relatively moderate effect of the phenol conversion for both pure zeolite and zeolite with added LM. This is consistent with relatively low influence of external diffusion on the overall reaction rate. Stirring rate does not also affect the selectivity of pure zeolite BEA. At the same time, a strong effect of stirring rate on the zeolite selectivity in the presence of LM is observed (**Figure S9, SI**). The selectivity gradually increases towards the O-acylation product as a function of stirring rate. The phenomenon can be attributed to more intensive contact between LM and acid sites at higher stirring rates. At lower stirring rates, LM which is much heavier than the zeolite is mostly localized in the bottom of catalytic reactor and does not efficiently interact with the zeolite active sites.

Pretreating zeolite BEA with LM could enhance LM's contact with the zeolite, leading to the formation of a composite LM-zeolite material. Indeed, treating zeolite BEA with an equivalent amount of LM at 175 °C results in the synthesis of a gray

material containing metal within the zeolite (**Figure S10, SI**). Testing this material in the acylation of phenol by hexanoic acid shows higher selectivity the O-acylation product compared to acylation without zeolite pretreatment by LM (**Figure S11, SI**).

2. Elucidating the promotion effects of LM in acylation reactions over zeolite

The SEM images (**Figure 5a**) show the presence of aggregates of BEA zeolite crystallites of about 75 nm. Zeolite after reaction in the presence of soldering alloy demonstrated metallic particles with a diameter 10-50 μm covered by zeolite crystallites (**Figure 5b-c, Figure S12, SI**). Furthermore, TEM analysis of the zeolite phase after reaction evidenced the presence of 1-3 nm alloy particles localized at the surface of zeolite particles (**Figure 5d**). According to TEM-EDX analysis, in addition to the presence of metal nanoparticles, a small fraction of metal is uniformly distributed on the zeolite BEA as very small nanoparticles (**Figure S13, SI**). According to the elemental analysis, the catalyst after the reaction in the presence of LM contained approximately 20 wt. % of alloy with a ratio of Pb and Sn similar to the parent alloy (**Table S1, SI**). Low temperature N_2 adsorption demonstrated a significant decrease in the specific surface area after the reaction for pure BEA zeolite and in the presence of alloy, which could be explained by blockage of the zeolite pores by carbon deposition (**Figure S14, SI, Table S1, SI**). There is no significant blockage of the pores of zeolite by pretreatment of fresh zeolite BEA in LM (Wood's/BEA) due to the high surface tension of the metal. This suggests relatively small penetration of LM into the zeolite pores.

These data confirm that a close contact between the zeolite and LM could lead to

specific interactions between zeolite and metal, affecting the selectivity, activity, and stability. The reaction of acylation with the use of bulky reagents most probably proceeds at the surface area of zeolites and at the entrance of the pores, where the effect of LM could be significant in comparison with the internal volume of zeolite where access of LM could be limited.

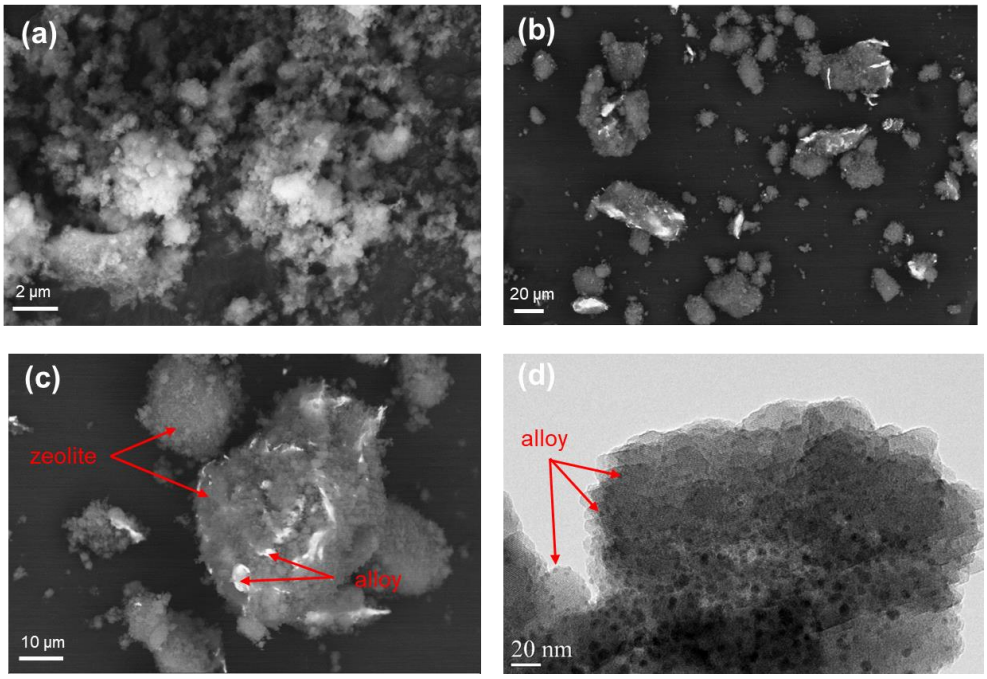

Figure 5. *SEM image of BEA zeolite (a), SEM (b,c) and TEM (d) images of the spent catalyst after phenol acylation by hexanoic acid over BEA zeolite with PbSn alloy.*

The increase in selectivity toward the O-acylation products was assigned earlier to the milder acidity of the catalysts [37]. It is possible that the presence of metal species in the vicinity of the Brönsted acid sites (BAS) could lead to the formation of cationic metal species or electronic interaction with the acid sites, thereby modifying their strength. The interaction of acid sites of zeolite BEA with LM has been examined using in situ FTIR spectroscopy in two series of experiments. The first series addressed the evaluation of acid sites in parent BEA and zeolite mixed with PbSn at 200 ^{o}C (sample

PbSn/BEA). The second 'dynamic' series simulates the dependence of acidity on reaction conditions as the spectra of the PbSn/BEA catalyst are collected at varying temperatures. **Figures 6** and **S15-S19, SI** present FTIR spectra of BEA and PbSn/BEA zeolites before and after Py adsorption.

Following the interaction between zeolite and LM (**Figure 6**), the relative peak intensity of isolated Si-OH and bridging Si-(OH)-Al groups, at 3745 and 3609 cm^{-1}, decreases while that of H-bound Si-OH groups, at ~3730 cm^{-1} increases. Such changes indicate partial dealumination of the BEA.

In addition, measured by Py adsorption, the concentration of BAS is lower and that of Lewis acid sites (LAS) is higher in PbSn/BEA compared to that of the parent zeolite (**Table S2, SI**). An even more pronounced decrease in the number of strong BAS is observed for the PbSn/BEA sample, particularly in the number of those located on the external surface of the zeolite (**Figure S18, SI**). This is further confirmed by the Py desorption data (**Figures 6, S16-S17, SI**), which show that only 27% of BAS of PbSn/BEA retain Py after its desorption at 400 ^{o}C as compared to ~40 % for the parent BEA. These results indicate a decrease in the strength of the acid sites in the presence of LM.

The 'dynamic' FTIR experiments show subtle changes in the OH region of the PbSn/BEA sample (**Figure S19, SI**). Minor, reversible shifts in both peak positions and intensities are observed when the sample temperature is raised from 100 to 200 °C, maintained at this level, and subsequently decreased back to 100 °C. Similar changes have been observed for the BEA sample, in agreement with Ref[33]. These data indicate that there are no further irreversible changes of the zeolite OH groups in the course of the simulated reaction, which could have resulted from the interaction between LM and

the zeolite. Overall, our FTIR data are consistent with the attenuation of acid site strength resulting from the interaction between zeolite and LM occurring in situ.

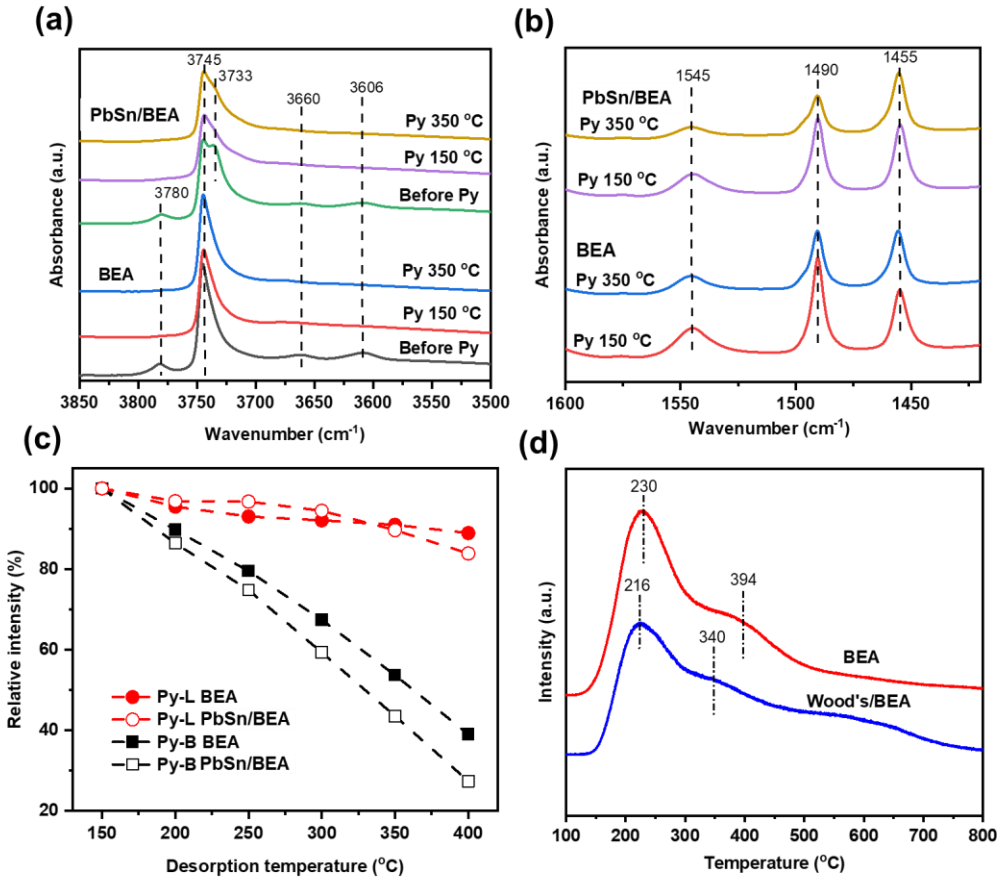

Figure 6. *(a, b) FTIR spectra of BEA and PbSn/BEA before Py adsorption and after Py desorption at 150 and 350 ºC. (c) Relative intensity of Lewis (L) and Brönsted acidity (B) during desorption of pyridine at different temperatures. (d) NH_3-TPD-MS (m/z=17) of BEA and Wood's/BEA catalysts*

NH_3-TPD has been used as an additional method to characterize the strength of the acid sites of zeolite BEA (**Figure 6**). The parent zeolite BEA exhibits the main peak of NH_3 desorption at 230 °C with a shoulder at 394 °C corresponding to strong acid sites. Conversely, the sample containing LM demonstrates a significant shift of the peak of strong acid sites to lower temperatures, indicating a decrease in the strength of acid sites. Interestingly, the total amount of acid sites in zeolite measured by NH_3-TPD is only slightly affected by exposure to LM.

This decrease in the strength of the acid sites in the presence of LM explains the selective O-acylation of phenols in comparison with C-acylation requiring stronger acidity. The interaction of LM particles with acid sites of zeolite could lead to the transfer of electronic density from LM to protons resulting in a decrease of the strength of the acid sites. This is consistent with the FTIR and NH_3-TPD showing the attenuation of the zeolite acidity and with catalytic tests demonstrating modification of the reaction selectivity in the presence of the LM alloy. A possible explanation for the observed increase of the catalyst stability could be due to the modification of the catalyst acidity and the decrease in the residence time of the acylated products over acid sites because of the competition with LM. It should also affect the selectivity by decrease of the probably of Fries rearrangement of esters. The recent assignment of Ga interaction with acid sites has been shown to increase the stability of ZSM-5 zeolite during the MTO reaction [38]. Thus, mixing non-metallic catalysts with low-melting-point metal can be a powerful tool to control the activity, selectivity and stability of the catalysts.

Conclusion

Our data demonstrate that the conducting catalytic reaction in LM results in major modification of the activity, selectivity and stability of the BEA zeolite catalysts.

In the presence of liquid metal alloys, the acylation of phenol results in the stable and selective formation of esters. In the absence of LM, BEA zeolite showed poor stability and produced mostly C-acylated products. The observed changes in the catalytic performance could be explained by the decrease in the strength of the zeolite Brønsted acid sites due to their continuous interactions with LM occurring in situ during the reaction. Using LM as a medium in the reactor has great potential to improve selectivity and catalyst stability of numerous catalytic reactions.

Supporting Information

GC images; substrate scope; test with PbSn; stability; analysis of deactivated catalyst by TGA, FTIR, GC-MS; effect of LM content; effect of stirring rate; photo of LM/BEA material and its catalytic performance; low temperature N_2 adsorption; FTIR Py adsorption.

Acknowledgements

We gratefully acknowledge the financial support of SATT Nord, Region Hauts-de-France and Bpifrance for this project.

References

1. Regan, C. K.; Craig, S. L.; Brauman, J. I., Steric effects and solvent effects in ionic reactions. *Science* **2002,** *295* (5563), 2245-2247.
2. Huxoll, F.; Jameel, F.; Bianga, J.; Seidensticker, T.; Stein, M.; Sadowski, G.; Vogt, D., Solvent selection in homogeneous catalysis—optimization of kinetics and reaction performance. *ACS Catalysis* **2020,** *11* (2), 590-594.
3. Shuai, L.; Luterbacher, J., Organic solvent effects in biomass conversion reactions. *ChemSusChem* **2016,** *9* (2), 133-155.
4. Mellmer, M. A.; Sener, C.; Gallo, J. M. R.; Luterbacher, J. S.; Alonso, D. M.; Dumesic, J. A., Solvent effects in acid-catalyzed biomass conversion reactions. *Angewandte chemie international edition* **2014,** *53* (44), 11872-11875.
5. Kalidas, C.; Hefter, G.; Marcus, Y., Gibbs energies of transfer of cations from water to mixed aqueous organic solvents. *Chemical Reviews* **2000,** *100* (3), 819-852.
6. Schäffner, B.; Schäffner, F.; Verevkin, S. P.; Börner, A., Organic carbonates as solvents in synthesis and catalysis. *Chemical Reviews* **2010,** *110* (8), 4554-4581.
7. Wasserscheid, P.; Keim, W., Ionic liquids—new "solutions" for transition metal catalysis. *Angewandte Chemie International Edition* **2000,** *39* (21), 3772-3789.
8. Dyson, P. J.; Jessop, P. G., Solvent effects in catalysis: rational improvements of catalysts via manipulation of solvent interactions. *Catalysis Science & Technology* **2016,** *6* (10), 3302-3316.
9. Mehnert, C. P.; Cook, R. A.; Dispenziere, N. C.; Afeworki, M., Supported ionic liquid catalysis − A new concept for homogeneous hydroformylation catalysis. *Journal of the American Chemical Society* **2002,** *124* (44), 12932-12933.
10. Muzart, J., Ionic liquids as solvents for catalyzed oxidations of organic compounds. *Advanced Synthesis & Catalysis* **2006,** *348* (3), 275-295.
11. Pârvulescu, V. I.; Hardacre, C., Catalysis in ionic liquids. *Chemical Reviews* **2007,**

107 (6), 2615-2665.
12. Liang, S.-T.; Wang, H.-Z.; Liu, J., Progress, mechanisms and applications of liquid-metal catalyst systems. *Chemistry – A European Journal* **2018,** *24* (67), 17616-17626.
13. Daeneke, T.; Khoshmanesh, K.; Mahmood, N.; de Castro, I. A.; Esrafilzadeh, D.; Barrow, S. J.; Dickey, M. D.; Kalantar-zadeh, K., Liquid metals: fundamentals and applications in chemistry. *Chemical Society Reviews* **2018,** *47* (11), 4073-4111.
14. Zhi, X.; Xie, F.; Zavabeti, A.; Li, G. K.; Harvie, D. J.; Kashi, E.; Batterham, R. J.; Liu, J. Z., Fundamentals, applications, and perspectives of liquid metals in catalysis: An overview of molecular simulations. *Energy & Fuels* **2023,** *37* (23), 17875–17891.
15. Daeneke, T.; Khoshmanesh, K.; Mahmood, N.; De Castro, I. A.; Esrafilzadeh, D.; Barrow, S.; Dickey, M.; Kalantar-Zadeh, K., Liquid metals: fundamentals and applications in chemistry. *Chemical Society Reviews* **2018,** *47* (11), 4073-4111.
16. Zuraiqi, K.; Zavabeti, A.; Allioux, F.-M.; Tang, J.; Nguyen, C. K.; Tafazolymotie, P.; Mayyas, M.; Ramarao, A. V.; Spencer, M.; Shah, K., Liquid metals in catalysis for energy applications. *Joule* **2020,** *4* (11), 2290-2321.
17. Taccardi, N.; Grabau, M.; Debuschewitz, J.; Distaso, M.; Brandl, M.; Hock, R.; Maier, F.; Papp, C.; Erhard, J.; Neiss, C.; Peukert, W.; Görling, A.; Steinrück, H. P.; Wasserscheid, P., Gallium-rich Pd–Ga phases as supported liquid metal catalysts. *Nature Chemistry* **2017,** *9*, 862.
18. Jakuttis, M.; Schönweiz, A.; Werner, S.; Franke, R.; Wiese, K.-D.; Haumann, M.; Wasserscheid, P., Rhodium–phosphite SILP catalysis for the highly selective hydroformylation of mixed C4 feedstocks. *Angewandte Chemie International Edition* **2011,** *50* (19), 4492-4495.
19. Armbrüster, M.; Kovnir, K.; Behrens, M.; Teschner, D.; Grin, Y.; Schlögl, R., Pd−Ga intermetallic compounds as highly selective semihydrogenation catalysts. *Journal of the American Chemical Society* **2010,** *132* (42), 14745-14747.
20. Gu, B.; Bahri, M.; Ersen, O.; Khodakov, A.; Ordomsky, V. V., Self-regeneration of cobalt and nickel catalysts promoted with bismuth for non-deactivating performance in carbon monoxide hydrogenation. *ACS Catalysis* **2019,** *9* (2), 991-1000.
21. Ordomsky, V. V.; Luo, Y.; Gu, B.; Carvalho, A.; Chernavskii, P. A.; Cheng, K.; Khodakov, A. Y., Soldering of Iron Catalysts for Direct Synthesis of Light Olefins from Syngas under Mild Reaction Conditions. *ACS Catalysis* **2017,** *7* (10), 6445-6452.
22. Delgado, J. A.; Claver, C.; Castillón, S.; Curulla-Ferré, D.; Ordomsky, V. V.; Godard, C., Fischer–Tropsch synthesis catalysed by small TiO2 supported cobalt nanoparticles prepared by sodium borohydride reduction. *Applied Catalysis A: General* **2016,** *513*, 39-46.
23. Rahim, M. A.; Tang, J.; Christofferson, A. J.; Kumar, P. V.; Meftahi, N.; Centurion, F.; Cao, Z.; Tang, J.; Baharfar, M.; Mayyas, M., Low-temperature liquid platinum catalyst. *Nature Chemistry* **2022,** *14* (8), 935-941.

24. Taccardi, N.; Grabau, M.; Debuschewitz, J.; Distaso, M.; Brandl, M.; Hock, R.; Maier, F.; Papp, C.; Erhard, J.; Neiss, C., Gallium-rich Pd–Ga phases as supported liquid metal catalysts. *Nature Chemistry* **2017,** *9* (9), 862-867.
25. Datta, R. S.; Syed, N.; Zavabeti, A.; Jannat, A.; Mohiuddin, M.; Rokunuzzaman, M.; Yue Zhang, B.; Rahman, M. A.; Atkin, P.; Messalea, K. A., Flexible two-dimensional indium tin oxide fabricated using a liquid metal printing technique. *Nature Electronics* **2020,** *3* (1), 51-58.
26. Zavabeti, A.; Ou, J. Z.; Carey, B. J.; Syed, N.; Orrell-Trigg, R.; Mayes, E. L.; Xu, C.; Kavehei, O.; O'Mullane, A. P.; Kaner, R. B., A liquid metal reaction environment for the room-temperature synthesis of atomically thin metal oxides. *Science* **2017,** *358* (6361), 332-335.
27. Chen, C.-C.; Yeh, C.-C.; Chen, C.-H.; Yu, M.-Y.; Liu, H.-L.; Wu, J.-J.; Chen, K.-H.; Chen, L.-C.; Peng, J.-Y.; Chen, Y.-F., Catalytic growth and characterization of gallium nitride nanowires. *Journal of the American Chemical Society* **2001,** *123* (12), 2791-2798.
28. Paquette, L. A., Comprehensive Organic Transformations. *Angewandte Chemie* **1990,** *102* (8), 964-965.
29. Höfle, G.; Steglich, W.; Vorbrüggen, H., 4-Dialkylaminopyridines as highly active acylation catalysts. *Angewandte Chemie International Edition in English* **1978,** *17* (8), 569-583.
30. Bertin, J.; Kagan, H. B.; Luche, J. L.; Setton, R., Graphite electrolytic lamellar reagents in organic chemistry. Esterifications in the presence of graphite bisulfate. *Journal of the American Chemical Society* **1974,** *96* (26), 8113-8115.
31. Corma, A.; Garcia, H.; Iborra, S.; Primo, J., Modified faujasite zeolites as catalysts in organic reactions: Esterification of carboxylic acids in the presence of HY zeolites. *Journal of Catalysis* **1989,** *120* (1), 78-87.
32. Le, S. D.; Nishimura, S.; Ebitani, K., Direct esterification of succinic acid with phenol using zeolite beta catalyst. *Catalysis Communications* **2019,** *122*, 20-23.
33. Zholobenko, V.; Freitas, C.; Jendrlin, M.; Bazin, P.; Travert, A.; Thibault-Starzyk, F., Probing the acid sites of zeolites with pyridine: Quantitative AGIR measurements of the molar absorption coefficients. *Journal of Catalysis* **2020,** *385*, 52-60.
34. Murashige, R.; Hayashi, Y.; Ohmori, S.; Torii, A.; Aizu, Y.; Muto, Y.; Murai, Y.; Oda, Y.; Hashimoto, M., Comparisons of O-acylation and Friedel–Crafts acylation of phenols and acyl chlorides and Fries rearrangement of phenyl esters in trifluoromethanesulfonic acid: effective synthesis of optically active homotyrosines. *Tetrahedron* **2011,** *67* (3), 641-649.
35. Neves, I.; Jayat, F.; Magnoux, P.; Pérot, G.; Ribeiro, F. R.; Gubelmann, M.; Guisnet, M., Acylation of phenol with acetic acid over a HZSM5 zeolite, reaction scheme. *Journal of Molecular Catalysis* **1994,** *93* (2), 169-179.
36. Padró, C. L.; Apesteguía, C. R., Acylation of phenol on solid acids: Study of the deactivation mechanism. *Catalysis Today* **2005,** *107-108*, 258-265.
37. Padró, C. L.; Apesteguía, C. R., Gas-phase synthesis of hydroxyacetophenones by acylation of phenol with acetic acid. *Journal of Catalysis* **2004,** *226* (2), 308-320.

38. Zhou, Y.; Santos, S.; Shamzhy, M.; Marinova, M.; Blanchenet, A.-M.; Kolyagin, Y. G.; Simon, P.; Trentesaux, M.; Sharna, S.; Ersen, O.; Zholobenko, V. L.; Saeys, M.; Khodakov, A. Y.; Ordomsky, V. V., Liquid metals for boosting stability of zeolite catalysts in the conversion of methanol to hydrocarbons. *Nature Communications* **2024,** *15* (1), 2228.